BEST AVAILABLE IMAGES

Defective images within this document are accurate representations of the original documents submitted by the applicant.

Defects in the images may include (but are not limited to):

- BLACK BORDERS
- TEXT CUT OFF AT TOP, BOTTOM OR SIDES
- FADED TEXT
- ILLEGIBLE TEXT
- SKEWED/SLANTED IMAGES
- COLORED PHOTOS
- BLACK OR VERY BLACK AND WHITE DARK PHOTOS
- GRAY SCALE DOCUMENTS

IMAGES ARE BEST AVAILABLE COPY.

As rescanning documents *will not* correct images, please do not report the images to the Image Problem Mailbox.

Photoinitiated Cationic Polymerization of Oxetane Formulated with Oxirane

HIROSHI SASAKI,[1]* JERZY M. RUDZIŃSKI,[2] and TOYOJI KAKUCHI[3]

[1]Tsukuba Research Laboratory, Toagosei Co. Ltd., 2 Ohkubo, Tsukuba, Ibaraki, 300-33, Japan; [2]Fujitsu Kyusyu System (FQS) Ltd., Hakataekimae-1, Hakata, Fukuoka, 812, Japan; [3]Division of Bioscience, Graduate School of Environmental Earth Science, Hokkaido University, Sapporo 060, Japan

SYNOPSIS

Photoinitiated cationic polymerization of oxetane, oxirane (epoxide), and a formulation of both was carried out and their reactivity compared. To investigate a formulated system of oxetane and oxirane in photoinitiated cationic polymerization, computational and experimental methods were used. In the computational study, we employed a semiempirical molecular orbital method (AM1). On the other hand, the reactivities of each system were evaluated and compared experimentally by a real-time FT-IR method. The computational study reveals that oxetane seems to polymerize in S_N2 mechaniam, but two possibilities, of S_N1 mechanism through the α-cleavage and of S_N2 mechanism through β-cleavage, are implied for oxirane. Using the real-time FT-IR method, the formulation of oxetane and oxirane was proved to possess rather high reactivities of oxetane toward photoinitiated cationic polymerization. The formulated system exhibited slightly lower number-average molecular weight than oxetane but higher than oxirane. These experimental observations are well explained in terms of the calculated reaction paths. © 1995 John Wiley & Sons, Inc.
Keywords: Oxetane • oxirane • photoinitiated cationic polymerization • semiempirical molecular orbital calculation • real-time FT-IR

INTRODUCTION

In recent years, photoinitiated cationic polymerization has become an important technique for the application and cure of coatings and adhesives because of its high throughput, low energy requirement, and the lack of a need for polluting solvents. Among many different types of monomers and oligomers: including vinyl ethers and oxiranes (epoxides). The photopolymerization of oxirane compounds provides coatings with high thermal capability, excellent adhesion, and good chemical resistance.[1,2] Although photopolymerized oxirane coatings are known for their high performance, commercially available oxiranes undergo photoinitiated cationic polymerization at rather slow rates. In some industrial applications, the low reactivity of these oxiranes has proved to be a considerable drawback to their use.[3] Thus, novel monomers that have the same performance capabilities as oxiranes but have higher reactivities are desired.

Three major factors contribute to the reactivity of heterocyclic monomers in the cationic ring-opening polymerization.[4] These are: (1) the nature of the heteroatom, its nucleophilicity, and its bond strength with the neighboring carbon atoms; (2) the ring strain; and (3) steric factors. It is interesting and informative to compare these factors for two classes of cyclic ethers: oxetanes and oxiranes. The ring strains of ethylene oxide and oxetane have been calculated to be 27.3 and 25.5 kcal/mol, respectively, and their pK_b values are 7.4 and 3.1, respectively.[5-7] Although both cyclic ethers have similar steric requirement and ring strains, the basicity of the oxetane is considerably greater than that of ethylene oxide. This latter parameter should, therefore, dominate in making the oxetanes more reactive than oxiranes in cationic ring-opening polymerizations. Considering this, we have synthesized a series of oxetanes and studied their reactivity toward photoinitiated cationic polymerization.[8-10] It was observed that the difunctional oxetanes are generally more reactive than their struc-

* To whom all correspondence should be addressed.

Journal of Polymer Science: Part A: Polymer Chemistry, Vol. 33, 1807–1816 (1995)
 CCC 0887-624X/95/111807-10

turally similar oxirane counterparts in photoinitiated cationic polymerization.

Previously, Saegusa et al. studied the cationic polymerization of various cyclic ether monomers and found that oxiranes work as promoters of oxetane polymerization using an authentic initiator such as $BF_3 \cdot Et_2O$.[11] From the discussion of the relationship between the yield of the resulting oxetane polymers and the polymerization temperature, they concluded that an initiator (acid) attacks a more reactive oxirane to readily generate an active species and the polymerization of oxetane occurs via an attack of the active species. Although details of the acceleration mechanism have not been revealed yet, application of the formulation of oxetane with oxirane to the photoinitiated cationic polymerization seems attractive.

To investigate the formulated system of oxetane and oxirane for photoinitiated cationic polymerization, we conducted theoretical and experimental studies. In the theoretical study, we employed the semiempirical molecular orbital method (AM1).[12] On the other hand, to study the reactivity experimentally, we decided to investigate not the yield of the polymer but the monomer conversion. A real-time IR method, which was developed by Decker, was introduced as an effective way to investigate the reactivity in photoinitiated polymerization.[13] Previously, we demonstrated the higher reactivity of novel oxetanes compared with that of oxiranes in the photoinitiated cationic polymerization using this method.[8,14] Recently, the real-time FT-IR method has also been proven to be effective and more precise for the investigation of fast photoinitiated polymerization by Yang.[15]

For the purpose of computational study, we chose methoxymethyl-oxirane (MeE) and 3-methyl-3-methoxymethyl-oxetane (MeO) as model compounds. In the real-time FT-IR study, we used 3-ethyl-3-phenoxymethyl-oxetane (PhO), phenoxymethyloxirane (PhE), and a diphenyl-4-thiophenoxyphenyl sulfonium hexafluoroantimonate (DTSH) as a cationic photoinitiator.

Monomers and photoinitiator

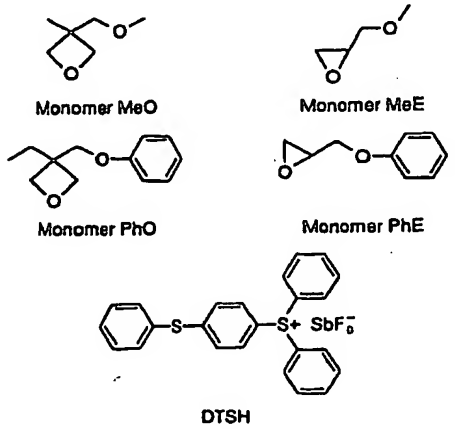

DTSH

Computational Technique

The semiempirical molecular orbital method (AM1)[12] implemented in the MOPAC'93[16] program was used throughout this study. ANCHOR II[17] served as a graphic user interface to model the structures, to run the calculation, and to analyze the results. In most cases of chain molecules having more then one stable conformation, the conformational potential energy surfaces (PES) were searched to determine the global energy minimum conformers. These were further used in the reaction coordinate calculation in the search of appropriate saddle points (transition state structures). The resulting structures were gradient optimized, then normal coordinate analyses were performed to check whether they represented true transition states (one negative eigenvalue of the Hessian). In most cases, the intrinsic reaction coordinate (IRC) calculations were done to correlate the transition states with corresponding energy minima (reactants and products).

EXPERIMENTAL

Monomers and Photoinitiator

Phenoxymethyl oxirane (PhE) was purchased from Tokyo Kasei Co. All other starting materials and solvents were reagent quality and were used as received. 3-Ethyl-3-(phenoxymethyl)-oxetane (PhO) was prepared from the phase-transfer reaction of 3-(chloromethyl)-3-ethyl-oxetane and phenol. Diphenyl-4-thiophenoxyphenyl sulfonium hexafluoroantimonate (DTSH) used as a photoinitiator was prepared using the procedures of Crivello.[18]

Polymerization and Real-Time FT-IR Measurement

The conversions of monomers to polymers were examined using real-time FT-IR spectroscopy employing the method of Yang.[15] The apparatus used for these measurements consisted of a Nicolet Magna-IR 550 FT-IR spectrometer that was equipped with a Ushio Spot Cure UIS-25102 (250 W) fitted with an optic fiber cable. The probe of the optic fiber cable was positioned so that the UV irradiation was directed onto the sample. Polymerizations were carried out at room temperature on samples of the monomers containing 0.5 mol % DTSH coated onto an aluminum plate (sample thickness = 10 μm). All the samples were irradiated at UV intensities of 44.2 mW/cm^2 in order to obtain sufficient spectra during the photopolymerization.

UV irradiation intensity measurements were made with the aid of a Ushio UNIMETER UIT-102 radiometer at 365 nm. During the irradiation, the decreases in the absorbance at 995 cm^{-1} for the oxetane and at 865 cm^{-1} for the oxirane were monitored. After the decrease in absorbance had ceased, the conversions of the monomers were calculated by comparing the initial and final absorbances.

Photopolymerization for GPC measurement

The photopolymerization was carried out under the same conditions as noted above. The irradiation time was 30 s for full conversion of monomers and the total irradiated energy was 1.33 J/cm^2. After irradiation, the resulting polymer was dissolved in THF containing a small amount of ammonium hydroxide (to neutralize acid). The molecular weight distribution was measured using gel permeation chromatography (GPC) in THF at 40°C on a TOSOH S8010 GPC system equipped with five polystyrene gel columns [TSK Gel G-7000HXL, 5000HXL, 4000HXL, MHXL (2 columns)] and a refractive index detector. The number-average molecular weight (M_n) was calculated from GPC curves on the basis of the polystyrene calibration.

RESULTS AND DISCUSSION

In the cationic ring-opening polymerization of cyclic ethers the propagation reaction can be described as a nucleophilic substitution of monomers with positively charged active species. The reaction can be classified into two types; the S_N2 type, in which the new bond is being formed and the old bond is being broken simultaneously, or the S_N1 type, in which the old bond is broken first, with the formation of a carbenium ion, which then immediately reacts with the monomer. The latter mechanism will be favored if the structure of the monomer is such that the resulting carbenium ion is stabilized and if the monomer is a weak nucleophile.

Previously, acid catalyzed substitution of cyclic ethers by various nucleophiles has been studied in detail. In the study of the effect of the rate of hydrolysis of oxetane and epichlorohydrin, Duffy found that the volume of activation was negative, and suggested an S_N2 for these reactions.[19] Parker studied the structure of the reaction product of chloride ion with oxirane species possessing various substituents in water and concluded that, depending on the structure of the substituents, the reaction underwent an S_N2 or a "borderline" S_N2, which means a mixture of S_N1 and S_N2.[20,21] The nucleophiles used in these studies, such as hydroxy ion or chloride, are stronger than cyclic ethers and, therefore, it does not seem proper to adapt these results to the cationic ring opening polymerization directly.

If the propagation reaction goes through an S_N2, an oxonium cation should exist during polymerization, but if it goes through an S_N1, a carbenium cation is generated. During cationic ring-opening polymerization of tetrahydrofuran, which possesses much lower ring-strain energy and higher nucleophilicity than oxirane, the existence of a trialkyloxonium cation was observed directly by ^1H and ^{13}C NMR.[22] In contrast to the tetrahydrofuranium cation, the oxiranium cation has never been directly observed in any polymerization process. Analysis of the isomerized side products, as well as studies of the stereochemistry of polymerization, indicate that carbenium ions may play a certain role in the polymerization of highly strained three-membered cyclic ethers, where the ring strain may facilitate the unimolecular opening of the oxonium ion ring. Based on his study of the polymerization of 1,2-anhydrosugars, Schuerch proposed a mechanism that includes the participation of carbenium ion type active species to explain the racemization through polymerization.[23] So far, no direct evidence has been shown for the participation of carbenium ions in the propagation reaction of the cyclic ethers.

The polymerization mechanism of oxiranes and/or oxetanes is still obscure and not as well documented as the polymerization of tetrahydrofuran.

Results of the AM1 Calculation

Ring-Opening Reaction

Ring-Opening Reaction of Protonated Oxirane (MeE). In the substituted protonated MeE, the two C—O bonds are not equivalent and the substituted one is weaker as manifested by its length, 1.547 Å vs. 1.511 Å (Scheme 1). The bond cleavage of the longer bond occurs much easier. The AM1-calculated energy barrier is lower for the substituted C—O bond by 8.66 kcal/mol. Moreover, the carbenium ion produced by the cleavage of the substituted bond is more stable (by 16.43 kcal/mol) than the one formed by cleavage of the unsubstituted bond (Scheme 1). The formation of the former carbenium ion results in the stabilization of the system (by 12.09 kcal/mol), while the formation of the latter results in destabilization (by 4.34 kcal/mol). This result shows that the cleavage of C—O bond should occur on the α-carbon (α-cleavage) and the ring

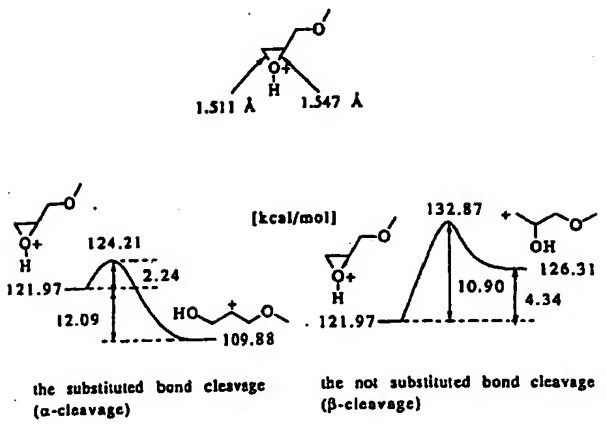

Scheme 1. Reaction diagram of ring-opening reaction of protonated oxirane (MeE).

opening of oxirane itself occurs easily to generate the carbenium ion.

Ring-Opening Reaction of Protonated Oxetane (MeO). The AM1-calculated energy barrier to the ring opening of the protonated MeO amounts to 14.84 kcal/mol, which is nearly seven times that for oxirane (2.24 kcal/mol), and the process results in the formation of a primary carbenium ion less stable than the reactant by 13.74 kcal/mol (Scheme 2). Ring opening of the protonated oxirane yielded a more stable secondary carbenium ion that was relative to the reactant on the potential energy scale. These results show that the generation of a primary carbenium ion from the oxetane ring seems difficult both thermodynamically and kinetically.

Propagation Stage

Protonated PhE and Neutral Monomer. The propagation stage of MeE via S_N1 mechanism: the carbenium ion formed by the ring opening of the protonated MeE is stabilized by another molecule of MeE through the addition of the carbenium ion site to the lone pair of the oxygen atom of the other molecule. The reaction diagram is shown in Scheme 3. This process is barrierless, and the stabilization amounts to 31.75 kcal/mol. The product of this stabilization may undergo a further ring opening (the energy barrier is 1.68 kcal/mol relative to the energy of the adduct) to give another carbenium ion that is more stable than the adduct by 12.19 kcal/mol and that undergoes a conformational change producing further stabilization by 15.27 kcal/mol.

The propagation stage of MeE on the α-carbon via S_N2 mechanism: the initial step of polymerization of MeE via the S_N2 mechanism involving protonated and neutral molecules of MeE can be viewed as an attack by the oxygen atom of the neutral species on the carbon atom of the protonated species. There are two possible sites on the protonated monomer: the substituted carbon (α-carbon) and the nonsubstituted carbon (β-carbon). The reaction diagram in Scheme 4 illustrates the energy change in the reaction pathway for the α-cleavage. The energy and bond lengths changes during the reaction are summarized in Table I. The changes in the bond length on the reaction coordinate indicate that it is not a clear S_N2 mechanism, but rather a two-step process in which the oxirane ring of the protonated species breaks first, giving a carbenium ion that is then stabilized with essentially zero energy barrier by the neutral molecule giving a dimer. Although the total stabilization energy is the same as for S_N1 (43.84 kcal/mol, quoted above), the energy barrier is lower: 0.58 kcal/mol as compared to 2.24 kcal/mol for ring opening in the isolated species.

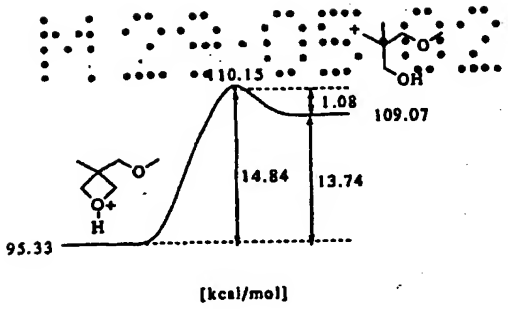

Scheme 2. Reaction diagram of ring-opening reaction of protonated oxetane (MeO).

The propagation stage of MeE on the β-carbon via S_N2 mechanism: the reaction diagram in Scheme 5 shows the energy change in the reaction pathway

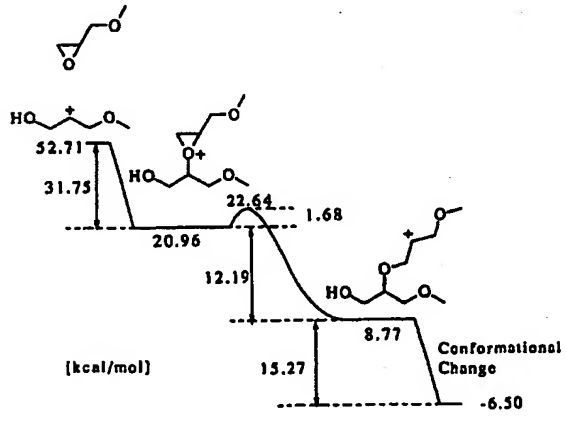

Scheme 3. Reaction diagram of second initiation stage of oxirane (MeE) through S_N1 mechanism.

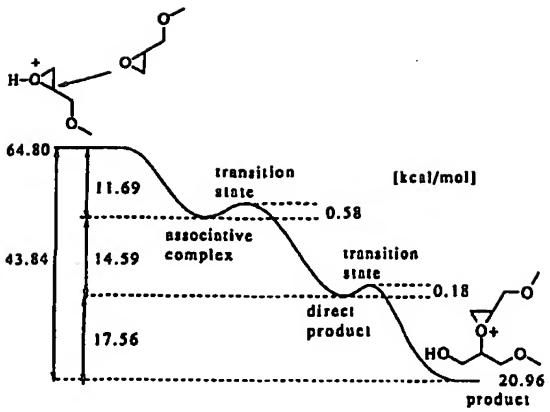

Scheme 4. Reaction diagram of second initiation stage of oxirane (MeE) through S_N2 mechanism on the α-carbon.

for the β-cleavage. The calculated transition state structure was correlated with the corresponding associative complex (reactant side) and the product in IRC calculation from the saddle point. The reaction pathway, which can be viewed by changes in the distances of the formed and cleaved bonds, proceeds from the reactants (separated by an infinite distance) to the associative complex, which is 10.23 kcal/mol lower in energy than the reactants. In the associative complex, the bond to be cleaved is slightly longer than in the reactant from 1.511 Å to 1.537 Å (Table I). The energy barrier is 3.30 kcal/mol relative to the energy of the associative complex and 6.93 kcal/mol lower than the sum of the energies of the reactants. At the transition state, the bond being cleaved is 1.847 Å and the one being formed 2.331 Å. The product of this reaction is 32.52 kcal/mol more stable relative to the potential energy of the reactants. The cleaved C—O bond distance is now 2.394 Å and the new O—C bond is 1.467 Å. The energy barrier calculated for the formation of a dimer via the S_N2 mechanism is less than zero relative to the energy contribution of the reactants (isolated species, not the associative complex).

The dimer formation between protonated MeE and MeO via S_N1 mechanism: the dimer formation between protonated MeE and neutral MeO is represented here as a two-step reaction. First, the protonated oxirane molecule undergoes ring opening to produce a carbenium ion, and then the carbenium ion is stabilized without an energy barrier by the neutral oxetane molecule. Scheme 6 shows the energetics of this process. The stabilization amounts to 37.87 kcal/mol and is 6.12 kcal/mol bigger than for the oxirane attack (31.75 kcal/mol).

The dimer formation between protonated MeE and MeO via S_N2 mechanism: the reaction diagram (Scheme 7) illustrates the energy and bond length changes in the reaction pathway for the dimer formation of protonated MeE attacked by MeO through the S_N2 path. Similarly to the propagation reaction of MeE, the changes in the bond length on the reaction coordinate indicate that it is not a clear S_N2 mechanism but rather a two-step process through a carbenium ion producing a dimer. Although the total stabilization energy is the same as for S_N1 quoted above, the energy barrier is lower: 0.55 kcal/mol as compared to 2.24 kcal/mol for the ring opening of the isolated species.

Protonated Oxetane and Neutral Monomer. The polymerization of MeO via S_N2 mechanism: the initial step of the acid-catalyzed polymerization of oxetanes via the S_N2 mechanism involving protonated and neutral molecules can be viewed as an attack of the oxygen atom of the neutral species on one of the two ring carbon atoms of the protonated species. In this model compound, the oxetane molecule is substituted in the 3-position; thus, the two-ring carbon atoms adjacent to the ring oxygen atom should be equivalent for the S_N2 attack, provided that the conformation of the side chain at the 3-position does not hinder the two carbon atoms. Scheme 8 shows the AM1-calculated energetics of the S_N2 pathway involving one protonated and one neutral MeO. The energy and the bond length changes during the reaction are also summarized in Table II. The calculated transition state structure was correlated with the corresponding associative complex and the product by IRC calculation from the transition state. The structures of associative complex, transition state, and direct product are shown in Figure 1. The reaction pathway proceeds from the reactants to the associative complex, which is 6.29 kcal/mol lower

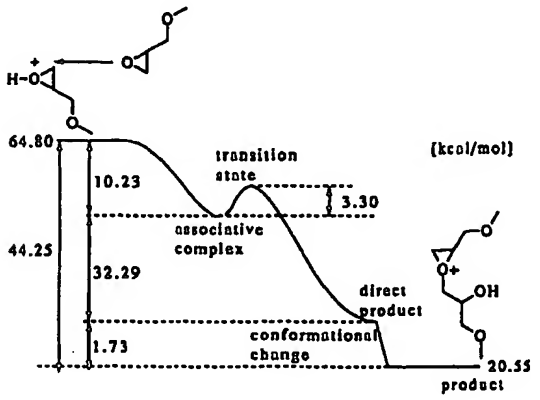

Scheme 5. Reaction diagram of second initiation stage of oxirane (MeE) through S_N2 mechanism on the β-carbon.

Table I. Changes of Heat of Formation and Bond Lengths during the Second Initiation Step of Oxirane (MeE) in AM1 Calculated S_N2 Attack on α- and β-Carbon Atoms

	α Cleavage			β Cleavage		
	ΔH_f[a]	Cleaved Bond[b]	Formed Bond[b]	ΔH_f[a]	Cleaved Bond[b]	Formed Bond[b]
Associative Complex	0.00	1.568	2.743	0.00	1.550	3.033
Transition State	0.58	1.737	2.444	3.30	1.993	2.221
Direct Product	−14.59	2.444	2.503	−32.29	2.611	1.475
Transition State	−14.41	2.419	2.100	—	—	—
Product	−32.15	2.342	1.479	−34.02	2.396	1.466

[a] Relative energy to the heat of formation of the associative complex; in kcal/mol.
[b] Bond length, in Å.

in energy than the reactants. In the associative complex, the bond to be cleaved is slightly longer than in the reactant. The energy barrier is 0.17 kcal/mol lower than the energy of reactants, but it is 6.12 kcal/mol above the associative compound. At the transition state, the bond being cleaved is 1.993 Å and the one being formed is 2.221 Å. The product of this reaction is 29.17 kcal/mol more stable on the potential energy scale relative to the reactants, and the cleaved C—O bond distance in the product is 2.611 Å, and the new O—C bond is 1.475 Å. Close look at the Figure 1 reveals that the structure of the associative complex undergoes not only a motion associated with the changes in the bond lengths in the reaction center on the way to transition state, but also a rotation along with the axis defined by the three atoms directly involved in the reaction (O—C—O). It should be noted, however, that because the structure of the associative complex is a direct result of the IRC calculation from the saddle point (transition state), it makes this structure unique in a sense of being one of the best candidates for the reaction to begin, among other possible associative complexes that could be drawn for the two reacting species on the reactant side.

Possible Polymerization Pass

The AM1 calculation of the ring-opening reaction of protonated oxirane indicate that the α-cleavage, generating a secondary carbenium cation stabilized by 12.0 kcal/mol from the reactant with an energy barrier of only 2.2 kcal/mol, seems to occur easily. In addition, the calculation of an S_N2 on the α-carbon of oxirane results in the spontaneous ring opening of the protonated oxirane ring on the α-carbon associated with the attacking monomer. On the other hand, the propagation reaction on the β-car-

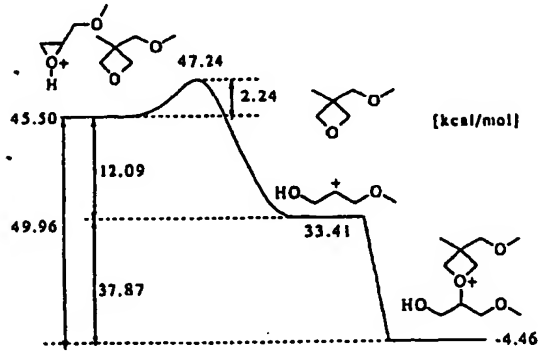

Scheme 6. Reaction diagram of second initiation stage of oxirane MeE attacked by oxetane (MeO) through S_N1 mechanism.

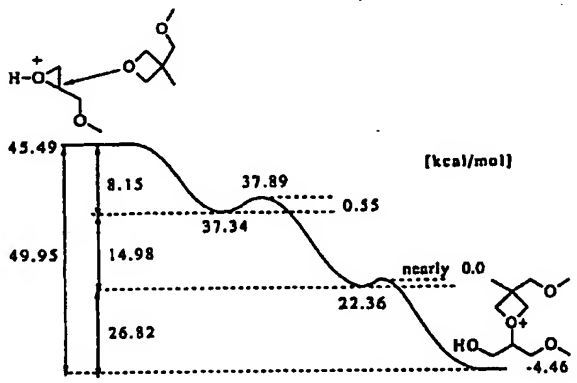

	associative complex (ac)	transition state (ts)	direct product (dp)	(ts)	product (pr)
cleaved bond	1.572	1.733	2.424		2.399
formed bond	2.705	2.596	2.389		1.481

Scheme 7. Reaction diagram and bond length change of second initiation stage of oxirane (MeE) attacked by oxetane (MeO) through S_N2 on the α-carbon.

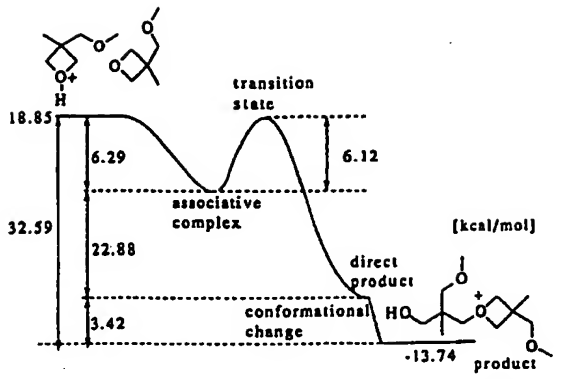

Scheme 8. Reaction diagram of second initiation stage of oxetane (MeO) through S_N2 mechanism.

bon of oxirane seems to go through S_N2. The former two calculation results imply that the propagation of oxirane proceeds in an S_N1 or an S_N1-like (in the presence of the attacking monomer) reaction if the ring-opening reaction occurs on the α-carbon on the oxirane ring.

The AM1 calculation of the ring opening reaction of protonated oxetane reveals that spontaneous ring opening, generating a rather unstable primary carbenium ion, seems unlikely to happen and that the polymerization of oxetanes through a S_N1 mechanism seems difficult both thermodynamically and kinetically. The propagation reaction of oxetane through S_N2 process results in the favorable energy and bond length changes on the reaction pathway. These results suggest that the propagation reaction of oxetane can be best viewed as an S_N2 ring opening of the positively charged oxetane species.

Real-Time FT-IR Method

Measurements on PhO and PhE

Figure 2 shows plots for the conversions of PhO, PhE vs. irradiated time, using the real-time FT-IR method. For the polymerization of oxetane PhO, possessing the same phenyl group as PhE, the conversion curve of the oxetanyl group showed an S-type curve indicative of induction time up to 2 s of UV irradiation and reached 80% conversion after 5 s. Scheme 9 explains the cationic ring-opening polymerization mechanism of cyclic ether through S_N2. In the initiation stage, first, an acid attacks a cyclic ether and generates a dialkyl oxonium cation in equilibrium reaction. Another monomer attacks this dialkyl oxonium cation in S_N2 and results in a trialkyl oxonium cation. Once the trialkyl oxonium cation is generated, the

Table II. Changes of Heat of Formation and the Bond Length during the Second Initiation Step of Oxirane (MeE) in AM1 Calculated S_N2 Mechanism

	ΔH_f[a]	Cleaved Bond[b]	Formed Bond[b]
Associative Complex	0.00	1.550	3.033
Transition State	6.12	1.993	2.221
Direct Product	−22.88	2.611	1.475

[a] Relative energy to the heat of formation of the associative complex, in kcal/mol.
[b] Bond length, in Å.

propagation goes through S_N2. Because the protonation of the cyclic monomer is in equilibrium, the ring-opening reaction of the dialkyl oxonium cation (generation of a trialkyl oxonium cation) is believed to be the rate-determining step of the initiation stage. The trialkyl oxonium cation is an actual propagating species, and the overall polymerization rate is governed by the generation rate of the trialkyl oxonium cation (i.e., the concentration of the cation). In the AM1 calculation of oxetane MeO, the polymerization path of the oxetane seems to go through S_N2. The induction time of PhO can be explained by the first step of the initiation stage of S_N2 (generation of the dial-

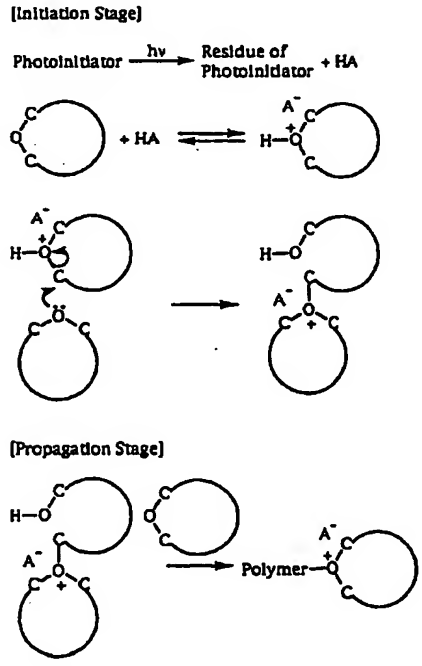

Scheme 9. Initiation and propagation reaction scheme of cyclic ether through S_N2 in the cationic polymerization.

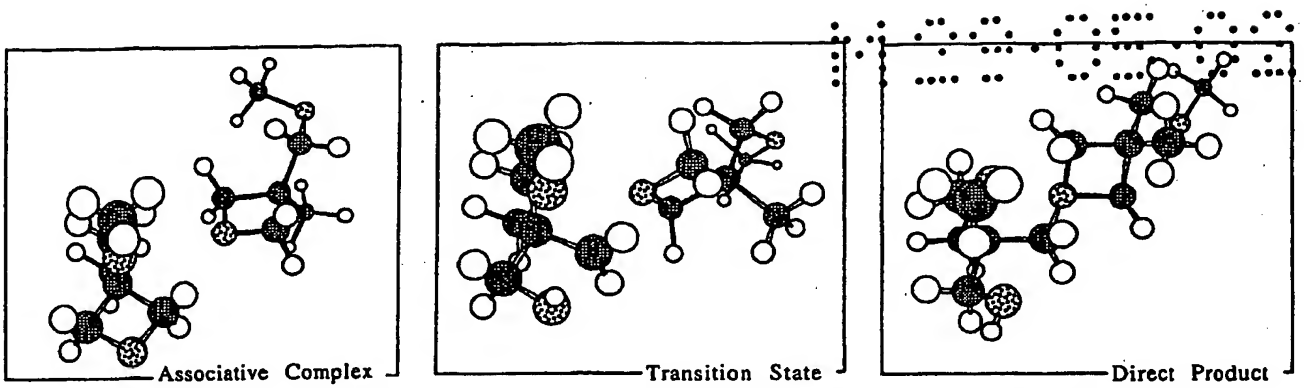

Figure 1. The AM1-calculated structures of the associative complex, transition state, and direct product on reaction passway for second initiation stage of oxetane (MeO) through S_N2 process.

kyloxonium cation in equilibrium). After generation of enough reactive chain ends (trialkyloxonium cation), the propagation stage of PhO proceeds smoothly, exhibiting a rather high polymerization rate due to its high basicity.

On the other hand, PhE exhibited a different conversion curve. No induction period was seen and initially it had a steeper slope indicative of a high reactivity than PhO. After 1 s of irradiation (around 10% conversion), the polymerization rate suddenly slowed down and the final conversion reached only around 30% after 5 s of irradiation. In the AM1 calculation of oxirane (MeE), both possibilities of an S_N1 (or an S_N1-like) through the α-cleavage and of an S_N2 through β-cleavage are implied. The absence of induction time indicates a fast initiation reaction, which might be explained by the spontaneous ring opening of the oxirane ring without an equilibrium reaction of the dialkyl oxonium cation and direct generation of a carbenium ion. The sudden drop in the polymerization rate might be explained by the stabilization of the carbenium ion by the open chain ether oxygen atom on the resulting polymer main chain due to the low basicity of the oxygen atom on the oxirane ring.

Measurements of Formulated Monomers

Figure 3 shows the time conversion curves of the oxetanyl ring on the photopolymerization of formulated monomers: 5 or 10 mol % of PhE in PhO. Although we also attempted to measure the absorbance change in the characteristic bands of the oxirane ring, the band height was so small in the formulated monomers that no accurate result was available. Upon addition of either 5 or 10 mol % of PhE, the conversion curves of the oxetanyl group exhibited very steep slopes indicative of a very high polymerization rate, and almost no

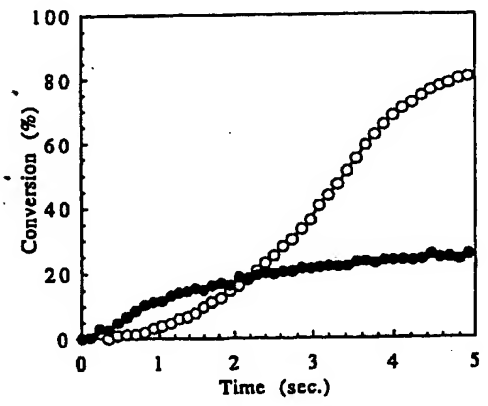

Figure 2. Conversion vs. irradiation time curves for PhE (●) and PhO (○) using 0.5 mol % photoinitiator at a UV intensity of 44.2 mW/cm^2.

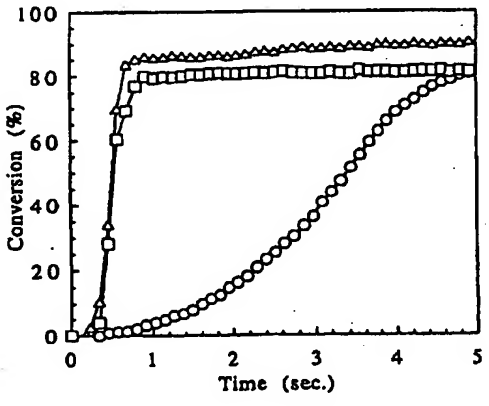

Figure 3. Conversion vs. irradiation time curves for PhO (○), PhO/PhE=95/5 (△), and 90/10 (□) using 0.5 mol % photoinitiator at a UV intensity of 44.2 mW/cm^2.

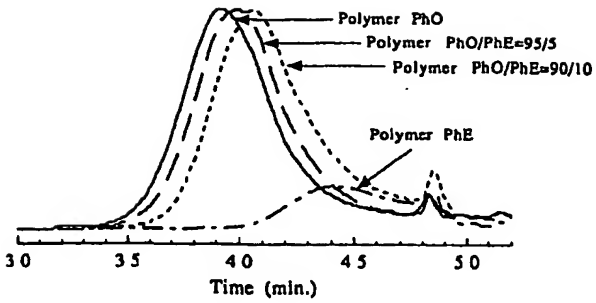

Figure 4. GPC elution curves of polymer PhO, PhE, and formulation using 0.5 mol % photoinitiator at a UV intensity of 44.2 mW/cm^2 and total irradiated energy of 1.33 J/cm^2.

induction period was seen. At less than 1 s of UV irradiation, the polymerization was almost completed, and the final conversion reached around 80%.

As previously noted in the homopolymerization of PhE, at least some portion of protonated PhE might generate a carbenium ion directly through the α-cleavage. This acceleration mechanism can be explained by the fast generation of a carbenium ion from the oxirane ring and of an active species, the trialkyloxonium cation. Once enough of the active species is generated, the polymerization of PhO proceeded smoothly to high conversion.

GPC Measurement

The GPC curves are shown in Figure 4. The polymer from PhE exhibited low M_n; around 2,400 at the peak top. On the other hand, the M_n of the polymer from PhO was relatively high; M_n = 13,900 at the peak top. The addition of PhE made the M_n lower, 11,100 for 5 mol % of PhE and 7,980 for 10 mol %. The low M_n of PhE might be explained by a chain transfer reaction or back biting, resulting in a cyclic oligomer during polymerization because of the low basicity of the oxygen atom on the oxirane ring. The higher M_n of PhO might reflect the nature of an S_N2, less chain transfer reaction, caused by the high basicity of the oxygen atom on the oxetane ring.

As previously noted, in the early stage of polymerization, oxirane generates carbenium ion and, by the attack of the oxetanyl group, a trialkyloxonium cation; the active species for an S_N2. In the formulated system, the number of active chain ends might be higher than in the polymerization of PhO alone. The lower M_n of the formulated polymer might be explained by this higher content of active species.

CONCLUSIONS

Results of the computational study suggest that the cationic ring-opening polymerization pathway of oxetane proceeds through an S_N2 mechanism. For oxirane, MeE, both possibilities of an S_N1 through the α-cleavage and of an S_N2 through the β-cleavage are implied.

Using a real-time FT-IR method, the formulation of oxetane and oxirane was proved to possess rather high reactivities of oxetane toward photoinitiated cationic polymerization. The oxetane polymer exhibited higher M_n than oxirane, and the formulated monomers showed slightly lower M_n than the oxetane, but higher M_n than the oxirane polymer. These experimental results are well explained by the calculated reaction path.

REFERENCES AND NOTES

1. J. V. Crivello and J. H. W. Lam, ACS Symposium Series, Vol. 114, American Chemical Society, 1979, p. 1.
2. J. V. Crivello, J. L. Lee, and D. A. Conlon, *J. Rad. Cur.*, **1**, 6 (1983).
3. F. Sitek, *Radcure Eur. '87*, 274 (1987).
4. S. Penczek, P. Kubisa, and K. Matyjaszewski, *Adv. Polym. Sci.*, **37**, 5 (1980).
5. A. S. Pell and G. Pilcher, *Trans. Faraday Soc.*, **61**, 71 (1965).
6. Y. Yamashita, T. Tsuda, M. Okada, and S. Iwatsuki, *J. Polym. Sci., Part A-1*, **4**, 2121 (1966).
7. S. Searles, M. Tamres, and E. R. Lippincott, *J. Am. Chem. Soc.*, **75**, 2775 (1953).
8. H. Sasaki and J. V. Crivello, *J. Macromol. Sci., Pure Appl. Chem.*, **A29**, 10, 915 (1992).
9. J. V. Crivello and H. Sasaki, *J. Macromol. Sci., Pure Appl. Chem.*, **A30**(2 & 3), 173 (1993).
10. J. V. Crivello and H. Sasaki, *J. Macromol. Sci., Pure Appl. Chem.*, **A30**(2 & 3), 189 (1993).
11. T. Saegusa, H. Imai, S. Hirai, and J. Furukawa, *Kogyo Kagaku Zassi*, **66**, 474 (1963).
12. M. J. S. Dewar, E. G. Zoebisch, E. F. Healy, and J. J. P. Stewart, *J. Am. Chem. Soc.*, **107**, 3902 (1985).
13. C. Decker and K. Moussa, *J. Polym. Sci., Part A: Polym. Chem.*, **28**, 3429 (1990).
14. H. Sasaki and J. V. Crivello, *Radtech North Am. '92*, 518 (1992).
15. D. B. Yang, *J. Polym. Sci., Part A: Polym. Chem.*, **31**, 199 (1993).

16. MOPAC'93, J. J. P. Stewart and Fujitsu Limited, Tokyo, Japan. see MOPAC'93 Manual and references cited there in.
17. ANCHOR II® is a molecular design support system for SUN® computers developed by Fujitsu Ltd. and Kureha Chemical Industry Co. Ltd., 1994.
18. S. R. Akhtar, J. V. Crivello, and J. L. Lee, *J. Org. Chem.*, 55(13), 4222 (1990).
19. W. J. le Noble and M. Duffy, *J. Phys. Chem.*, 68(3), 619 (1964).
20. J. K. Addy and R. E. Parker, *J. Chem. Soc.*, 915 (1963).
21. J. K. Addy and R. E. Parker, *J. Chem. Soc.*, 644 (1965).
22. K. Matyjaszewski and S. Penczek, *J. Polym. Sci., Polym. Chem. Ed.*, 12, 1905 (1974).
23. J. Zachoval and J. Schuerch, *J. Polym. Sci. C*, 28, 187 (1969).

Received November 3, 1994
Accepted January 17, 1995